J Mater Sci: Mater Med (2013) 24:2171–2180
DOI 10.1007/s10856-013-4972-8

Bioactivity and cytotoxicity of glass and glass–ceramics based on the $3CaO{\cdot}P_2O_5$–SiO_2–MgO system

Juliana K. M. F. Daguano · Sizue O. Rogero · Murilo C. Crovace · Oscar Peitl · Kurt Strecker · Claudinei dos Santos

Received: 7 February 2013 / Accepted: 31 May 2013 / Published online: 14 June 2013

Abstract The mechanical strength of bioactive glasses can be improved by controlled crystallization, turning its use as bulk bone implants viable. However, crystallization may affect the bioactivity of the material. The aim of this study was to develop glass–ceramics of the nominal composition (wt%) $52.75(3CaO{\cdot}P_2O_5)$–$30SiO_2$–17.25MgO, with different crystallized fractions and to evaluate their in vitro cytotoxicity and bioactivity. Specimens were heat-treated at 700, 775 and 975 °C, for 4 h. The major crystalline phase identified was whitlockite, an Mg-substituted tricalcium phosphate. The evaluation of the cytotoxicity was carried out by the neutral red uptake methodology. Ionic exchanges with the simulated body fluid SBF-K9 acellular solution during the in vitro bioactivity tests highlight the differences in terms of chemical reactivity between the glass and the glass–ceramics. The effect of crystallinity on the rates of hydroxycarbonate apatite (HCA) formation was followed by Fourier transformed infrared spectroscopy. Although all glass–ceramics can be considered bioactive, the glass–ceramic heat-treated at 775 °C (V775-4) presented the most interesting result, because the onset for HCA formation is at about 24 h and after 7 days the HCA layer dominates completely the spectrum. This occurs probably due to the presence of the whitlockite phase ($3(Ca,Mg)O{\cdot}P_2O_5$). All samples were considered not cytotoxic.

J. K. M. F. Daguano (✉) · C. dos Santos
Departamento de Engenharia de Materiais, Escola de Engenharia de Lorena, Universidade de São Paulo, Lorena, SP, Brazil
e-mail: ju_daguano@yahoo.com.br

S. O. Rogero
Instituto de Pesquisas Energéticas e Nucleares, São Paulo, SP, Brazil

M. C. Crovace · O. Peitl
Laboratório de Materiais Vítreos, Departamento de Engenharia de Materiais, Universidade Federal de São Carlos, São Carlos, SP, Brazil

K. Strecker
Universidade Federal de São João del-Rei, Campus Sto Antônio, Praça Frei Orlando 170, Centro, São João del-Rei, MG, Brazil

C. dos Santos
Centro Universitário de Volta Redonda, UNIFOA, Campus Três Poços, Volta Redonda, RJ, Brazil

1 Introduction

The development of glass–ceramic materials for biomedical purposes greatly increased in the recent decades [1–3]. A bioactive glass–ceramic is one that has a specific biological response at the interface of the implant, resulting in the formation of a strong bond between material and tissue [4]. This connection between the implant and tissue is primarily due to the occurrence of various biophysical and biochemical reactions at the interface of the material, producing a biologically active layer of hydroxycarbonate apatite (HCA), which is responsible for the strong bond between tissue and implant material. It is also known that, besides connecting the implant with the bone, a layer of HCA is the most thermodynamically stable at the physiological pH of 7.4, which helps in maintaining the implant in the human body [5, 6]. In addition, bioactive glass–ceramics and bio-glasses exhibit other important properties in the bone healing process as they are also angiogenic [7–9], antimicrobial [10] and anti-inflammatory [11].

The biomaterials used as bone substitutes, besides being bioactive, should provide adequate mechanical properties and to be compatible with the tissue being replaced, with

good flexural strength and fracture toughness and a Young's modulus similar to that of bone tissue [12]. Normally these characteristics will be determined by the kind of application of the material, considering the mechanical stresses and the environment in which this material will be exposed daily. Thus, although the emergence of new bioactive materials is highlighted in recent years [13–15], there are still evident limitations regarding their mechanical properties, due to the high brittleness of ceramics [11]. Therefore, an alternative is the development of glass–ceramic materials which have both improved mechanical properties and high bioactivity [1]. The main method for the improvement of mechanical properties of bioglasses is by partial crystallization. However, it is known that an increased crystalline fraction may compromise its bioactivity and may even turn it into a bioinert material [16]. Thus, it is necessary for the development of an improved biomaterial, to balance these properties.

Studies on the effect of partial crystallization of glass–ceramics intended to improve the mechanical properties while maintaining the bioactivity, have been carried out [17–20]. Crystallization of the glass is extremely important for the improvement of the mechanical properties. It has been shown [16, 21] that bioglasses with high crystalline fractions exhibit a decrease in their biological performance, because the formation of the HCA layer is related to the amount of existing residual glassy phase, since its formation depends on the dissolution of calcium and silicon ions present in the glassy phase [6, 22]. On the other hand, the presence of crystalline phases which exhibit a moderate/high dissolution rate, such as wollastonite ($CaSiO_3$) [13], combeite ($Na_2Ca_2Si_3O_9$) [23] and tricalcium phosphate [$Ca_3(PO_4)_2$] [24], may play a role similar to that of a glassy phase as source of calcium and silicon ions, thus maintaining the bioactivity of the material. As example of glass–ceramics which exhibit good fracture toughness and high bioactivity are the so-called glass–ceramic A-W Cerabone® developed by Kokubo et al. [25], Bioverit developed by Holand and Vogel [26] and Biosilicate® developed by Peitl et al. [27].

The A-W Cerabone® glass–ceramic is obtained from the glass system MgO–CaO–SiO_2–P_2O_5 and contains two crystal phases, fluorapatite and β-wollastonite. The presence of these two phases ensures good fracture resistance, with fracture toughness close to 2.0 MPa $m^{1/2}$, because the apatite matrix reinforced by needle-like wollastonite crystals increase the energy necessary for crack propagation. On the other hand, this material exhibits an elastic modulus substantially higher than that of natural bone. In in vitro tests the development of a HCA layer occurred after 7 days of immersion in simulated body fluid (SBF) [21, 25]. Peitl et al. [16] studied the effect of crystallization on the formation of the HCA layer in Bioglass® 45S5, showing that the formation of HCA is delayed but not hindered, even after full crystallization. Furthermore, Matsumoto et al. [28] showed that Biosilicate® presents similar biological responses to autogenous bone grafts, but limited fracture toughness of 0.95 MPa $m^{1/2}$. However, these results were a significant evolution in the field of biomaterials, demonstrating the possibility of the materials development with good mechanical properties and still maintaining their biological performance or functionality [15].

Glass–ceramics from the 3CaO·P_2O_5–SiO_2–MgO system with different crystalline fractions have emerged as bone substitutes because of their interesting mechanical properties [12, 29], similar to natural bone tissue. In a previous work [12], it was shown that the phase transformations that occur in these materials during heat-treatment under different temperatures directly influence the microstructure and hence the mechanical properties. The effect of crystallization of bioglasses on the formation of HCA is still a controversial subject and for this glass system has not been explored yet.

The objective of this study was to investigate the effect of crystallization on the bioactivity of glass–ceramics from the system 3CaO·P_2O_5–SiO_2–MgO in order to advance the development of new bone substitutes. The biological behavior was evaluated by in vitro tests. The first requirement for a material to be bioactive and to bond to living bone tissue is the ability to form a layer of HCA on their surface [4]. This phenomenon can be reproduced in vitro and be evaluated using a solution that mimics the body fluid containing ion concentrations similar to blood plasma. A protein-free and acellular solution with ion concentrations similar to those of human blood plasma, SBF-K9, is the solution currently used in most in vitro tests [30]. The results of the bioactivity of the glass–ceramics after different immersion times in SBF are discussed in relation to their microstructural characteristics and degree of crystallinity, as well as the type of crystal phases formed. Additionally, in vitro cytotoxicity tests using the neutral red uptake method with NCTC clones L929 were conducted to evaluate the biocompatibility of the materials developed and their possible use as bone implants. Another issue addressed in this work was to evaluate the behavior of glasses with high MgO content (26.6 mol%). In glasses, the addition of MgO tends to diminish the bioactivity, however this behavior is questioned by some authors in previous studies [31, 32].

2 Experimental procedure

2.1 Preparation of glass and crystallization treatments

The bioglass of composition 52.75 wt% $Ca_3(PO_4)_2$–30 wt% SiO_2–17.25 wt% MgO was prepared from reagent-

grade $Ca(H_2PO_4)_2$, $CaCO_3$, SiO_2 and MgO. Batches of 100 g were obtained by mixing the raw materials in ethanol for 240 min, drying at 90 °C for 24 h and passing it through a sieve with openings of 64 μm for deagglomeration. The glass was prepared according to the conventional melting method in a platinum crucible at 1,600 °C, as described in Ref. [12]. Finally, the glass was cast into cylinders with 12 mm diameter in a stainless steel mould and annealed for 120 min at 700 °C (30 °C below the glass transition temperature—Tg of this glass) and slowly cooled down to room temperature. For crystallization, samples were further heat-treated at 700, 775 and 975 °C, for 4 h (V700-4, V775-4 and V975-4, respectively), and cooled down at a rate of 3 °C/min.

2.2 Characterization

In order to identify the crystalline phases, the heat-treated samples were analyzed by high resolution X-ray diffractometry (HRXRD), using a diffractometer with multiple axes, Hubber—Germany. The samples were crushed and sieved to a particle size smaller than 32 μm. The measurements were carried out in a set up of two coupled concentric circles ($\omega - 2\theta$), with a monochromatic X-ray beam of 10 keV ($\lambda = 1.2398$ Å). The powders were put in a cylindrical support of 10 mm diameter and 2 mm depth and were rotated in order to promote randomness of orientation of the crystallographic planes. The diffracted beam was collected by a germanium crystal (200) and a scintillation detector. The powders were analyzed under diffraction angles ranging from 7° to 50°, with a step size of 0.01° and a counting time of 1 s per step. The amount of the crystalline phases (crystallized volume fraction) contained in the glass–ceramic samples was determined according to the procedure used by Krimm and Tobolsky [33]. The percent crystallinity (IC) was calculated by the ratio of the crystalline area (A_C) and the total area (A_T = amorphous + crystalline), using

Origin software (OriginLab Corp., Northampton, MA) and the following equation:

$$IC = (A_C/A_T) \times 100 \quad (1)$$

2.3 In vitro bioactivity tests in SBF

The in vitro bioactivity of the glass and glass–ceramics, reflected in their ability of inducing hydroxyapatite formation on their surfaces, was investigated according to the method described by Kokubo et al. [30] and based on ISO 23317-07 [34], by immersion of bulk samples in SBF at 37 ± 0.1 °C. SBF is an acellular, protein-free solution with an ionic concentration (in mM) of 142.0 Na^+, 5.0 K^+, 2.5 Ca^{2+}, 1.5 Mg^{2+}, 147.8 Cl^-, 4.2 HCO_3^-, 1.0 HPO_4^{2-} and 0.5 SO_4^{2-}, buffered with tris-hydroxymethyl-aminomethane (Tris, 50 mM) and hydrochloric acid solutions. The SBF solution was adjusted to pH of 7.25, unlike a pH of 7.4 suggested by ISO 23317, since most of paper in the literature used this pH value [15, 16, 21, 22, 25, 30]. Cylinder shaped samples (ø 12 mm × 3 mm) were fixed along its circumference by a nylon string to allow for pellet suspension in the SBF solution during the test. The samples were cleaned for 15 s by ultrasound in acetone and, after drying, were soaked in sterilized polyethylene terephthalate bottles (PETs) containing the SBF solution.

The volume of SBF used in the bioactivity tests is related to the surface area of the sample. According to the procedures described by ISO 23317-07 [34], for a dense material, the appropriate volume of solution should obey the following relationship:

$$Sa/Vs = 0.1\ cm^{-1} \quad (2)$$

where Vs represents the volume of SBF (mL) and Sa represents the total geometric surface area of the sample (mm^2).

During the tests, the samples were kept in the SBF solution for 1, 3, 6, 24, 48, 72, 120, 168 and 336 h. After the test time required for each sample, they were removed from their bottles and immersed in acetone for 10 s to remove the SBF and stop surface reactions. After drying, both sample surfaces were analyzed to check for the formation of a HCA layer at the surface.

The monitoring of surface changes of the samples after the in vitro bioactivity tests was performed by Fourier transform infrared spectroscopy (FTIR) using a spectrometer PerkinElmer Spectrum GX model operating in reflectance mode with a 4 cm^{-1} resolution in the 4,000–400 cm^{-1} region. Morphological characterization of the samples regarding the surface changes that occurred during the in vitro bioactivity tests was analyzed by SEM. A set of samples was selected and analyzed before and after soaking in SBF solution at different testing times. The samples were coated with a thin evaporated gold layer, to turn the surface conductive, and then analyzed under a Phenom Scanning Electron Microscope—FEI, which aided the surface characterization through qualitative chemical analysis.

2.4 Cytotoxicity procedure

The in vitro biocompatibility of the glass and glass–ceramic samples were evaluated by a cytotoxicity assay as described by Daguano et al. [12]. These tests were performed for the powder samples according to ISO 10993-5 [35] by the neutral red uptake methodology.

Table 1 Phases analysis of the samples V700-4, V775-4 and V975-4

Samples	Heat-treatments	Phases	IC (%)
V700-4	700 °C/4 h	Amorphous	0
V775-4	775 °C/4 h	Amorphous + whitlockite [3(Ca, Mg)O·P_2O_5]	27
V975-4	975 °C/4 h	Amorphous + whitlockite [3(Ca, Mg)O·P_2O_5] + not cataloged silicate	63

3 Results and discussion

3.1 Characterization of the samples

In the Table 1 it can be observed the heat-treatments for obtaining the glass–ceramic samples, the phases identified in these materials by HRXRD and the percent of fraction crystallized (IC %).

The analysis by HRXRD allowed identifying typical behavior for an amorphous material of the sample V700-4, where no distinct diffraction peaks can be observed, only a "halo" characteristic of an amorphous phase. Moreover, the process of crystallization of the glass can be noted, as indicated by a decreasing amount of residual vitreous phase, i.e., an increase in IC % values of up to 63 %, and the formation of whitlockite [3(Ca,Mg)O·P_2O_5] at 775 °C and further formation of a "transient silicate" at 975 °C [12].

The glass–ceramics studied in this work, independent of the temperature of the thermal treatment, showed whitlockite (PDF # 87-1582) as the major crystalline phase. In this phase Mg is partially substituted by Ca, forming a solid solution of [3(Ca,Mg)O·P_2O_5]. At 975 °C, a second crystal phase has been detected. Even after thorough analysis of the database of cataloged crystalline phases, JCPDS, it was impossible to identify this phase. The formation of this silicate and its crystallization kinetics are not well understood. It is believed that this phase is a metastable phase [12], whose origin lay in the residual glass matrix after crystallization of whitlockite. Metastable crystalline phases are quite common as the initial formation of a crystal when a glass is subjected to a heat treatment [36].

3.2 Biological response—bioactivity tests

The structure of the 3CaO·P_2O_5–SiO_2–MgO glass, as represented by the FTIR spectrum shown in Fig. 1, is quite similar to the 45S5 Bioglass®. The 45S5 Bioglass is considered the reference material for these biomaterials and therefore was chosen as standard, because its reactivity in SBF solution has been extensively studied. Furthermore,

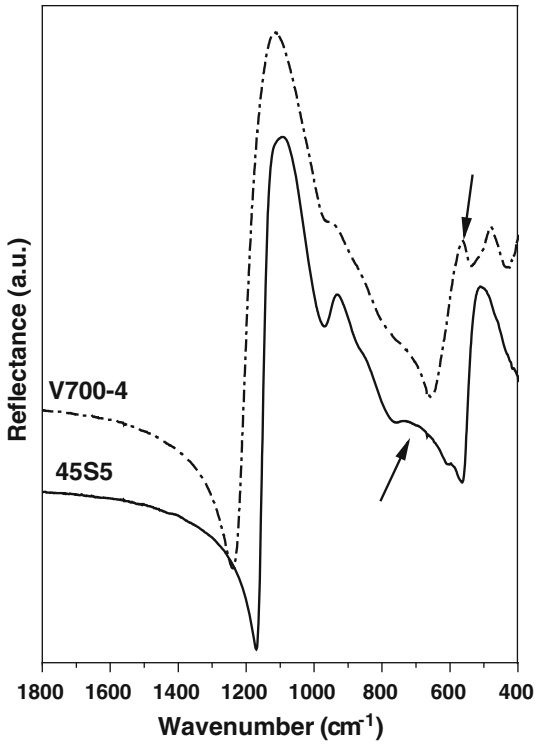

Fig. 1 Comparison of the structures of the glasses Bioglass 45S5 e V700-4 prior to immersion in SBF by FTIR spectroscopy

the mechanism of formation of HCA on its surface is well understood and is referred as the Hench's mechanism [37].

Some differences between these materials are shown by the highlighted bands at 565 and 950 cm^{-1}, corresponding to P–$O_{(b)}$ and Si–$O_{(NBO)}$ bonds, respectively. The peak at 565 cm^{-1} is stronger in the sample V700-4, because the composition studied in this work has a higher P_2O_5 (10.6 mol %) content compared to the 45S5 Bioglass (2.6 mol %). This higher P_2O_5 content in the sample V700-4 may also explain the difference found in the band at 950 cm^{-1}, being less intense in the sample V700-4. In this case, a higher P_2O_5 content provides a more interconnected glass network, because it acts as glass forming ions, removing ions that act as modifiers from the network (Na^+ and Ca^{2+}). In consequence, the number of non-bridging oxygen ions (NBO) decreases and, consequently, also the intensity of the band at 950 cm^{-1}, which corresponds to the Si–$O_{(NBO)}$ bonds.

The FTIR spectra of the glass V700-4 and glass–ceramics V775-4 and V975-4 after immersion in simulated body fluid for up to 14 days are shown in Fig. 2. As can be seen (Fig. 2a), the formation of an amorphous layer rich in Ca–P (stage 4, according to Hench's mechanism) occurs after a period of 2 days as indicated by the band in the range 530–610 cm^{-1}. After 5 days, the formation of HCA starts, characterized by the appearance of the double peak from P–$O_{(b)}$ bonds at 565 and 605 cm^{-1} and by the peak

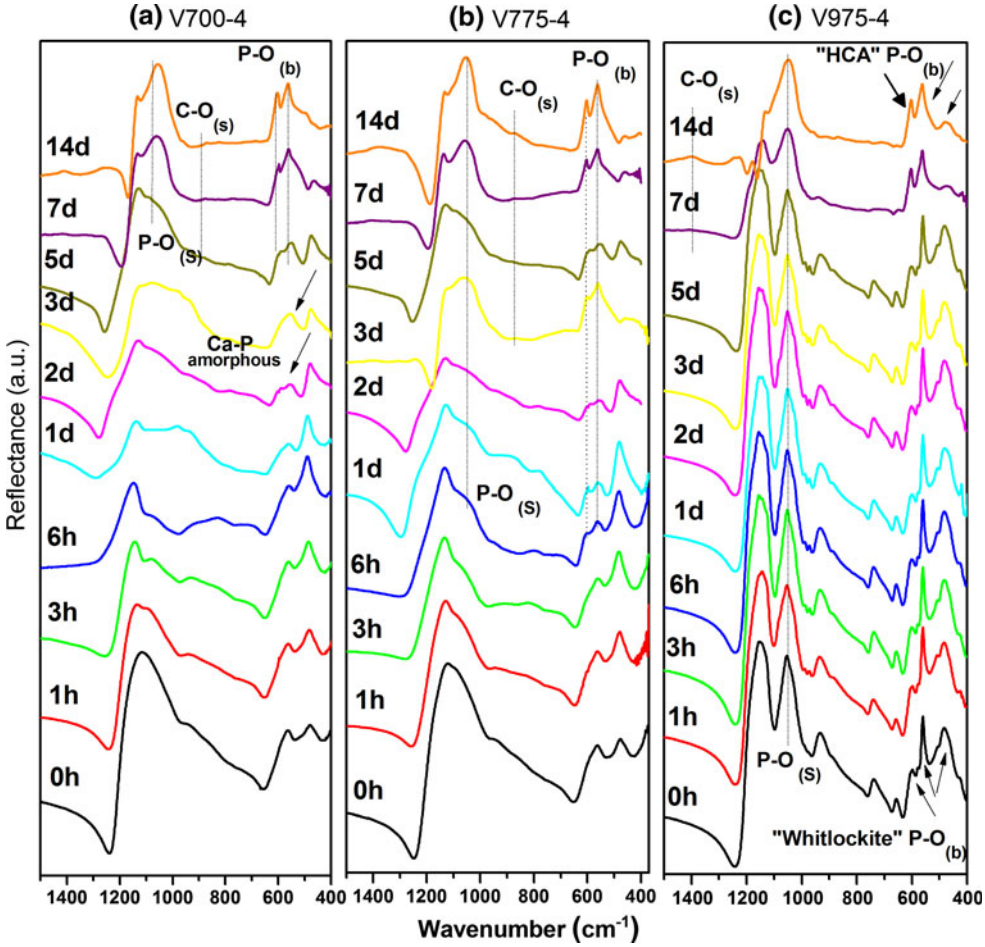

Fig. 2 FTIR spectra before and after immersion in SBF for up to 14 days of the **a** glass V700-4, **b** glass–ceramic V775-4 and **c** glass–ceramic V975-4

from the stretching of the $P–O_{(s)}$ bonds at 1,050 cm^{-1}. After 7 days the hydroxyapatite layer formed completely superimposes all peaks related to Si–O bonds (stage 5).

Evaluating the sequence of reactions observed during the formation of the HCA layer, it can be noted that the glass V700-4 follows the Hench mechanism. This statement is in agreement with a study by Oliveira et al. [31] of glasses of this system. However, the time required for the five stages of the Hench mechanism to occur is higher for the V700-4 glass investigated in this work in comparison to the 45S5 Bioglass, being 5 days for V700-4 and only 1 day for the 45S5 Bioglass, respectively.

The difference in the reactivity of these materials may be represented by the time necessary for polycondensation of the silanol groups to form a layer of silica gel (stage 3). For the glass V700-4 this happens in 3 h, characterized by bands at 540–415 and 1,250–1,095 cm^{-1}, whereas for Bioglass 45S5 the bands referring to silica gel are already visible after 1 h, see Fig. 3.

The role played by magnesium in the system $3CaO{\cdot}P_2O_5$–SiO_2–MgO for an improved bioactivity compensates the longer time necessary for the formation of the HCA layer. According to Oliveira et al. [31], magnesium promotes the breaking of Si–O–Si bonds and increases the amount of amorphous phase dispersed in the glass due to the disproportionation reaction $2Q^2 \rightarrow Q^0 + Q^4$. In turn, the glass matrix is more depolymerized with a higher content of morulae ($Q^0 = SiO_4^{-4}$) which enables increased leaching of the glass surface, and in consequence, the ion exchange of alkaline earth ions with H_3O^+ ions from the solution. Thus, the stages 1–3 can be accelerated by the presence of MgO.

Filgueiras et al. [38] state that the stages 1–3 are not significantly affected, but the stages 4 and 5 are retarded by the presence of magnesium in the SBF solution. Saboori et al. [32] reported that magnesium may inhibit crystallization of hydroxyapatite by replacing calcium in the structure or may induce the formation of low crystallinity hydroxyapatite. In higher concentrations magnesium may form amorphous calcium phosphate. However, in the current analysis we found that the formation of amorphous Ca–P was delayed. The crystallization of HCA was delayed as well, but not hindered.

Despite this, it is important to note the high bioactivity of glass V700-4 despite the slower formation of the HCA layer when compared to other glass–ceramic materials [4, 13, 20].

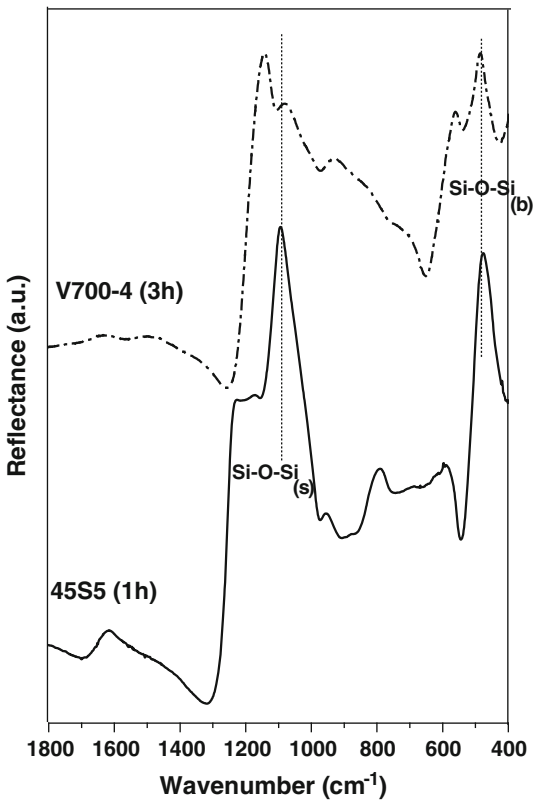

Fig. 3 FTIR spectra showing the formation of a silica gel layer on the surface of the Bioglass 45S50 after 1 h and the glass V700-4 after 3 h immersion in SBF

The steps of the HCA formation on the surface of the glass–ceramic V775-4, which contains approximately IC = 27 % of the crystal phase whitlockite, [3(Ca, Mg) $O.P_2O_5$]—β-TMCP, are shown in Fig. 2b. Due to the low crystallized fraction of the material, the sample V775-4 initially presents a FTIR spectrum similar to that of glass V700-4. The sequence of reactions during the in vitro analysis indicates that there is a different mechanism in the formation of HCA in this glass–ceramic, which occurs more rapidly than in the precursor glass V700-4.

Li et al. [22] state that a bioglass can be transformed into an inert material by crystallization, unless the glass–ceramic maintains a high amount of residual amorphous phase (>90 %). However, Peitl et al. [39] showed that glasses and glass–ceramics of composition Na_2O–2CaO–$3SiO_2$ show similar reactions forming HCA, indicating that crystallization does not significantly affect the reaction kinetics.

In the Fig. 2b, the formation of a layer of silica gel layer in sample V775-4 can be observed after 3 h, as indicated by the bands at 540–415 and 1,250–1,095 cm^{-1}, as for the glass V700-4. However, the formation of amorphous Ca–P occurred in a period of 6 h, characterized by a broad band at 565 cm^{-1}. The onset of HCA formation can be observed after a period of 1 day mainly by the band at 890–850 cm^{-1} related to $C–O_{(s)}$ bonds. Finally, after 7 days of exposure to SBF, the HCA layer completely covered the FTIR spectrum.

Despite the formation of the HCA, the silica gel layer can still be observed within 1 day (Fig. 2b). In fact, during the crystallization of HCA, both layers of calcium phosphate (amorphous and crystalline) are very close and the peaks are mixed with silica gel layer, but it is possible to follow this process by the bands from $Si–O–Si_{(b)}$ and $Si–O–Si_{(s)}$ bonds which broaden and decrease in intensity, respectively.

It is believed that the surprisingly rapid formation of the HCA layer in the glass–ceramic V775-4, 5 times as fast as in the precursor glass, is due to the presence of whitlockite. This relationship may be explained by two factors: (i) the whitlockite or β-TMCP phase is a more soluble phase, promoting a super-saturation in the local microenvironment and, as consequence, the crystallization of HCA and therefore presents higher bioactivity, (ii) the β-TMCP phase accelerates the crystallization of hydroxyapatite acting as a preferential site for nucleation and growth of HCA, due to characteristics of the surface [40].

These results are in accordance with recent studies which indicate that witlockite has significant biological affinity and activity, responding very well to physiological environments [41–45]. Kamitakahara et. al [43] reported that porous glass–ceramics containing whitlockite and diopside have high bioactivity and potential for bone repair, mainly compositions containing 60 and 50 % mass of whitlockite. The reason why apatite-forming ability increased with increasing β-TMCP in the glass composition is attributed to the easy release of calcium ions from the glassy phase in the glass–ceramics into the SBF. Thus, β-TMCP precipitated in the glass–ceramics may contributed little to the bioactivity, but the bioresorbability is induced by this phase. El-Meliegy and El-Bassyouni [44] showed that, for fluorophlogopite-whitlockite containing glass–ceramics, the compositions containing higher content of whitlockite showed the formation of a finely crystallized HA prior to the other compositions within 7 days of immersion in SBF. This HA layer was created favorably by heterogeneous precipitation from the solution, when it became supersaturated.

Banerjee et al. [45] studied the influence of MgO and SrO doping on the mechanical and biological properties of β-tricalcium phosphate (β-TCP) and demonstrated better cell attachment and proliferation for doped β-TMCP in vitro cell–material interaction study, also in vivo study established that bone formed more quickly in doped samples than in control.

The stages of the formation of the HCA layer on the surface of the glass–ceramic V975-4 were also evaluated during exposure in SBF and are shown in Fig. 2c. Analysis

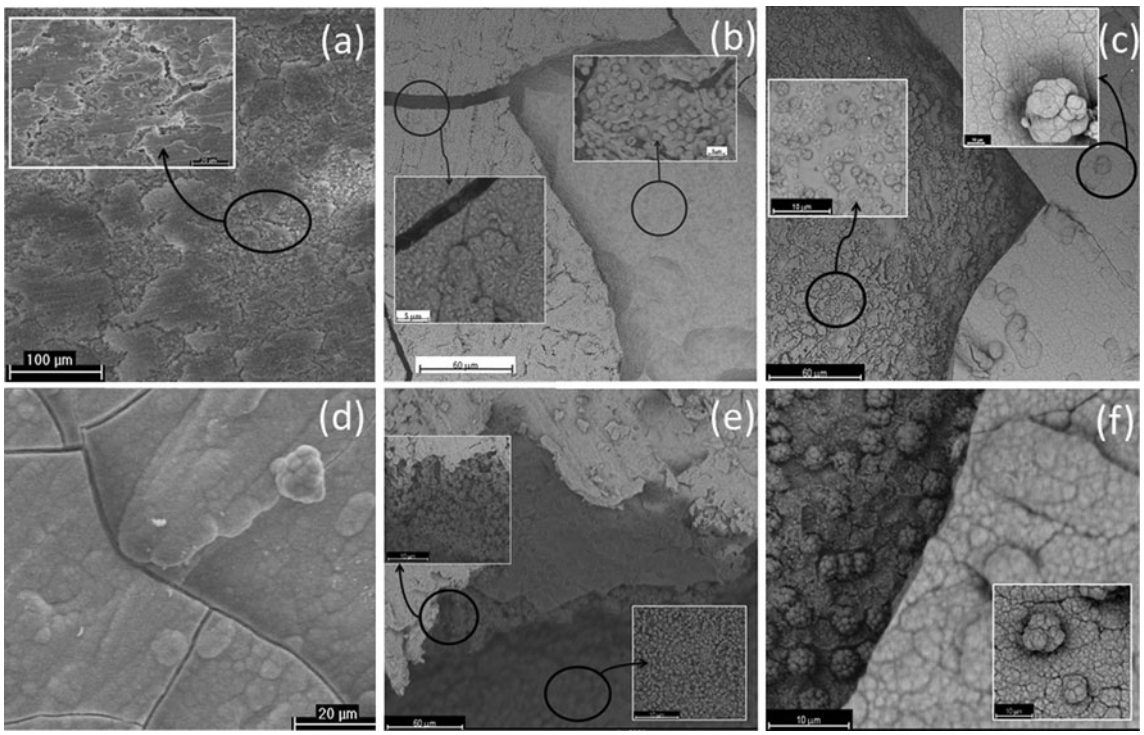

Fig. 4 SEM-micrograph of the surface of glass V700-4 and glass–ceramic V775-4 after immersion in SBF for: **a** 3 days, **b** 7 days and **c** 14 days **d** 3 days, **e** 7 days and **f** 14 days, respectively

of the sample V975-4 shows that the glass–ceramic is chemically more resistant, because the spectra shown are identical up to 5 days of exposure, always consisting of bands characterizing the partially crystallized material (IC $\approx$ 63 %). Some bands could be identified and correspond to the whitlockite phase as indicated in Fig. 2c. Still based on data obtained by FTIR analysis, the onset of HCA formations occurs at about 7 days and only after 14 days the HCA layer reins the spectrum.

After testing the bioactivity in SBF solution, the surfaces of the samples V700-4, V775 and V975-4-4 were observed by scanning electron microscopy, as shown in Figs. 4 and 5. The images confirm the formation of HCA and reveal details of this layer for each specific sample.

The structure of the apatite layer formed on the surface of the bioglass V700-4 and bioglass–ceramic V775-4 after immersion in SBF for 3, 7 and 14 days, can be observed in the Fig. 4. The structural features agree with the results obtained by FTIR analysis. After 3 days, a leaching of the sample surface of the V700-4 can be observed, due to the contact with the solution and consequent ion exchange. The corresponding FTIR spectrum indicates the presence of an amorphous film rich in Ca–P. Some regions of the surface such as the amplified detail shown in Fig. 4a, suggest the deposition of a film on the glass structure that has as main feature the presence of amorphous silica morulae.

After 7 days, the sample surface of the V700-4 was covered by a layer of globular crystals of HCA, as shown in detail in Fig. 4b, and confirmed by the FTIR spectrum of HCA. After 14 days, this layer has grown and is quite similar to that formed on Bioglass 45S5. Furthermore, a more globular shape of the hydroxyapatite and fibrils in its structure can be noted, characteristic of a highly crystalline apatite, Fig. 4c. In both cases, a region rich of SiO_2 morulae below these layers can be detected, suggesting that the morulae are not completely leached by the SBF solution, but are part of the silica gel layer formed by the condensation of silanol groups.

In fact, after 3 days, see Fig. 4d, the glass–ceramic V775-4 developed a well defined layer of HCA similar to that formed by Bioglass 45S5. In this way the glass–ceramic material V775-4 exhibits its great potential as bioactive material, superior to glass V700-4. In Fig. 4e, the material appears to be stratified into three planes: a lower plane, which would correspond to the layer of silica gel with incorporated morulae and a polymerized network; an intermediate plane corresponding to a film rich in CaP, and a top layer of HCA. Just small changes with increasing exposure time can be seen in the layer already formed; only the thickness of this layer increases for longer exposure in SBF, Fig. 4e, f.

Additionally, the surface of the glass ceramic V975-4 was analyzed by scanning electron microscopy after

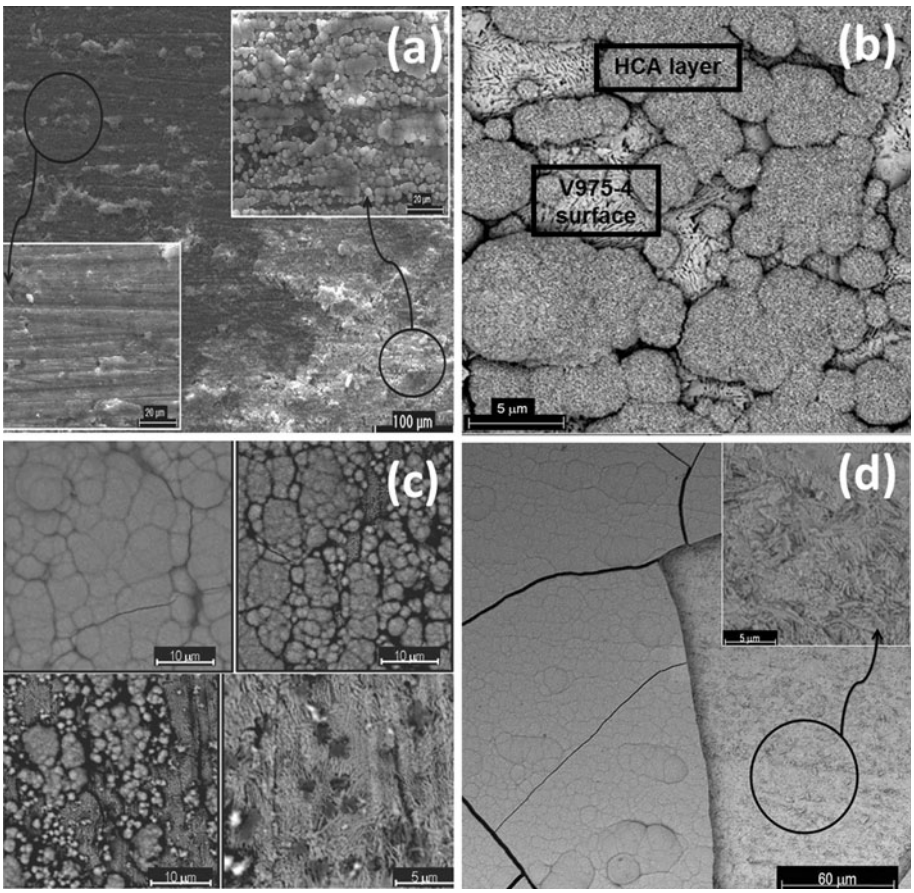

Fig. 5 SEM-micrograph of the surface of the glass–ceramic V975-4 after immersion in SBF for: **a** 3 days, **b** 5 days, **c** 7 days, **d** 14 days. Different features of the HCA layer formed can be observed at different regions of the surface of the glass–ceramic, primarily for (**c**)

in vitro tests, Fig. 5. These results are more informative than those shown by FTIR analysis and differ for the exposure period of 3 days. For this time of exposure the FTIR spectrum does not indicate the formation of HCA but closely observing the SEM micrographs in some regions globular structures can be detected, suggesting the presence of HCA on the materials surface, as shown in Fig. 5a. In other regions, the surface of the material appears to be unchanged, even risks caused by the grinding procedure during sample preparation are still detectable. From these images we can state that the formation of the HCA is very heterogeneous, making analysis difficult by technical FTIR. Thus, it is possible that the beam must be focused precisely on a region which had not HCA and their detection is not possible. While these globular structures do not appear homogeneously distributed, they have been clearly identified and may indicate the beginning of the formation of HCA. But further investigations are necessary to support this assumption.

The disparities between different regions of the material continue for exposure times of 7 and 14 days. In Fig. 5c it can be observed both the presence of a well developed thick layer of HCA and the presence of small globules of isolated HCA on the surface of the material. After 14 days, Fig. 5d, the layer is quite thick and apparently more homogeneous. It is believed that the formation of HCA occurs due to the presence of phase whitlockite and thus the observation of the heterogeneous layer.

Interestingly enough, neither FTIR, nor SEM analysis were able to detected the steps of the formation of the silica gel layer and the amorphous calcium phosphate in the glass–ceramic V975-4. In contradiction to the Hench's mechanism, it appears that the hydroxyapatite layer is formed directly on the glass-ceramic surface and in specific regions. Figure 5b highlights this behavior where globular structures of hydroxyapatite with fibrils, characteristic of a crystalline layer, can be identified, deposited on the surface of the leached glass-ceramic.

3.3 Cytotoxicity tests

The results for the evaluation of cytotoxicity of glass and glass–ceramics from the system $3CaO{\cdot}P_2O_5$–SiO_2–MgO by in vitro tests with fibroblast cells L-929, are shown in Fig. 6.

The analysis shows the percentage of cell viability for different extract concentrations. In general, satisfactory results were obtained because cell viability (percent), which quantifies the number of living cells after the

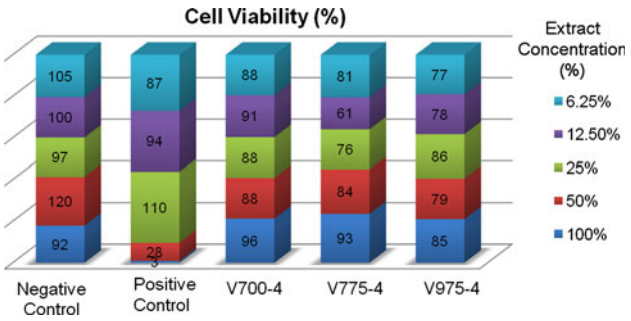

Fig. 6 Results of cytotoxicity tests by the neutral red dye uptake methodology

cytotoxicity test, was around 80 %, regardless of the extract concentration. The analyzed samples showed similar behavior, as this technique does not allow to affirm which of them has the greatest potential for medical applications, or to evaluate benefits of the crystallization process on the biological properties in regard to the glass. Values higher than 80 % are characteristic for an excellent non-cytotoxic material, meaning that this percentage of cells present in the beginning of the test remained alive.

4 Conclusions

Regarding the in vitro bioactivity test, it is still impossible to establish the mechanism of HCA formation, but it is already known that the glass–ceramic V975-4 based on $3CaO{\cdot}P_2O_5$–SiO_2–MgO-system may follow a different mechanism as that proposed by Hench. In the glass sample V700-4 the formation of an amorphous Ca–P layer after 48 h of exposition in SBF has been observed by FTIR analysis and also the onset for HCA formation after 5 days. The glass–ceramic V775-4 presented the most interesting result, because the onset for HCA formation is at about 24 h and after 7 days the HCA layer dominates the spectrum. This occurs probably due to the presence of the whitlockite phase. However, the analysis of the V975-4 sample is non conclusive, because the spectra are all quite similar until the end of the 5 day exposition. Based on the FTIR data, it was observed that the onset for HCA formation is about 7 days, and only after 14 days the HCA layer dominates the spectrum. There is an overlap of whitlockite and HCA peaks in the FTIR spectrum, which may interfere the results. The in vitro cytotoxicity test has shown that, regardless of the material's phase, all samples were not cytotoxic. Furthermore, a cell viability of about 80 % characterizes a great biocompatibility potential of the material.

Acknowledgments The authors acknowledge Prof. Dr. Edgar Dutra Zanotto for technical support, and FAPESP for financial support, under Grants Nos. 07/50510-4 and 2013/07793-6. Also we give our thanks to Clever R. Chinaglia and Bruno P. Rodrigues for the help provided during the development of the present work.

References

1. Hölland W. Biocompatible and bioactive glass-ceramics—state of the art and new directions. J Non-Cryst Solids. 1997;219:192–7.
2. Abo-Mosallam HA, Salama SN, Salman SM. Formulation and characterization of glass–ceramics based on $Na_2Ca_2Si_3O_9$–$Ca_5(PO_4)_3F$–Mg_2SiO_4-system in relation to their biological activity. J Mater Sci Mater Med. 2009. doi:10.1007/s10856-009-3811-4.
3. Salman SM, Salama SN, Darwish H, Abo-Mosallam HA. In vitro bioactivity of glass–ceramics of the $CaMgSi_2O_6$–$CaSiO_3$–$Ca_5(PO_4)_3F$–Na_2SiO_3 system with TiO_2 or ZnO additives. Ceram Int. 2009;35:1083–93.
4. Hench LL, West JK. Biological application of bioactive glasses. Life Chem Rep. 1996;13:187–241.
5. Wanpeng C, Hench LL. Bioactive Materials. Ceram Int. 1996;22:493–507.
6. Hoppe A, Güldal NS, Boccaccini AR. A review of the biological response to ionic dissolution products from bioactive glasses and glass-ceramics. Biomaterials. 2011;32:2757–74.
7. Day RM. Bioactive glass stimulates the secretion of angiogenic growth factors and angiogenesis in vitro. Tissue Eng. 2005;11:768–77.
8. Jell G, Stevens MM. Gene activation by bioactive glasses. J Mater Sci Mater Med. 2006;17:997–1002.
9. Hench LL. Genetic design of bioactive glass. J Eur Ceram Soc. 2009;29:1257–65.
10. Martins CH, Carvalho TC, Souza MGM, Ravagnani C, Peitl O, Zanotto ED, Panzeri H, Casemiro LA. Assessment of antimicrobial effect of Biosilicate® against anaerobic, microaerophilic and facultative anaerobic microorganisms. J Mater Sci Mater Med. 2011;22:1439–46.
11. Rahaman MN, Day DE, Bal BS, Fu Q, Jung SB, Bonewald LF, Tomsia AP. Bioactive glass in tissue engineering. Acta Biomater. 2011;7:2355–73.
12. Daguano JKMF, Santos C, Fernandes MHFV, Rogero SO, Strecker K. Effect of partial crystallization on the mechanical properties and cytotoxicity of bioactive glass from the $3CaO{\cdot}P_2O_5$–SiO_2–MgO system. J Mech Behav Biomed Mater. 2012;14:78–88.
13. Casa-Lillo MA, Velásquez P, De Aza PN. Influence of thermal treatment on the in vitro bioactivity of wollastonite materials. J Mater Sci Mater Med. 2011;22:907–15.
14. Murphy S, Boyd D, Moane S, Bennett M. The effect of composition on ion release from Ca–Sr–Na–Zn–Si glass bone grafts. J Mater Sci Mater Med. 2009;20:2207–14.
15. Tulyaganov DU, Agathopoulos S, Valerio P, Balamurugan A, Saranti A, Karakassides MA, Ferreira JMF. Synthesis, bioactivity and preliminary biocompatibility studies of glasses in the system CaO–MgO–SiO_2–Na_2O–P_2O_5–CaF_2. J Mater Sci Mater Med. 2011. doi:10.1007/s10856-010-4203-5.
16. Peitl O, LaTorre GP, Hench LL. Effect of crystallization on apatite-layer formation of bioactive glass 45S5. J Biomed Mater Res. 1996;30:509–14.
17. Clupper DC, Hench LL, Mecholsky JJ. Strength and toughness of tape cast bioactive glass 45S5 following heat-treatment. J Eur Ceram Soc. 2004;24:2929–34.
18. Kanchanarat N, Bandyopadhyay-Ghosh S, Reaney IM, Brook IM, Hatton PV. Microstructure and mechanical properties of fluorcanasite

glass-ceramics for biomedical applications. J Mater Sci. 2008;43:759–65.
19. Liporaci JLJ, Rosa AL, Beloti MM, Johnson A, Noort R, Barros VMR. In vitro osteogenesis on fluorcanasite glass-ceramic with three different chemical compositions. J Mater Sci Mater Med. 2008;19:833–8.
20. Bhakta S, Pattanayak DK, Takadama H, Kokubo T, Miller CA, Mirsaneh M, Reaney IM, Brook I, Noort R, Hatton PV. Prediction of osteoconductive activity of modified potassium fluorrichterite glass-ceramics by immersion in simulated body fluid. J Mater Sci Mater Med. 2010. doi:10.1007/s10856-010-4145-y.
21. Kokubo T. Bioactive glass-ceramics: properties and applications. Biomaterials. 1991;12:155–63.
22. Li P, Yang Q, Zhang F. The effect of residual glassy phase in a bioactive glass-ceramic on the formation of its surface apatite layer in vitro. J Mater Sci Mater Med. 1992. doi:10.1007/BF00701242.
23. Arstila H, Vedel E, Hupa L, Hupa M. Factors affecting crystallization of bioactive glasses. J Eur Ceram Soc. 2007;27:1543.
24. Kannan S, Goetz-Neunhoeffer F, Neubauer J, Pina S, Torres PMC, Ferreira JMF. Synthesis and structural characterization of strontium-and magnesium-co-substituted β-tricalcium phosphate. Acta Biomater. 2010;6:571–6.
25. Kokubo T, Ito S, Sakka S, Yamamuro T. Formation of a high-strength bioactive glass-ceramic in the system MgO–CaO–SiO_2–P_2O_5. J Mater Sci. 1986;21:536–40.
26. Holand W, Vogel W. Machinable and phosphate glass ceramics. In: Hench LL, Wilson J, editors. An Introduction to Bioceramics. Singapore: World Scientific; 1993. p. 125–37.
27. Peitl Filho O, Hench LL, La Torre G, Zanotto ED. Bioactive ceramics and method of preparing bioactive ceramics. US5981412; Nov. 1999.
28. Matsumoto MA, Caviquioli G, Biguetti CC, Holgado LA, Saraiva PP, Rennó AAM, Kawakami RY. A novel bioactive vitroceramic presents similar biological responses as autogenous bone grafts. J Mater Sci Mater Med. 2012. doi:10.1007/s10856-012-4612-8.
29. Daguano JKMF, Suzuki PA, Strecker K, Fernandes MHFV, Santos C. Evaluation of the micro-hardness and fracture toughness of amorphous and partially crystallized $3CaO{\cdot}P_2O_5$–SiO_2–MgO bioglasses. Mater Sci Eng, A. 2012;533:26–32.
30. Kokubo T, Takadama H. How useful is SBF in predicting in vivo bone bioactivity? Biomaterials. 2006;27:2907–15.
31. Oliveira JM, Correia RN, Fernandes MH. Effects of Si speciation on the in vitro bioactivity of glasses. Biomaterials. 2002;23:371–9.
32. Saboori A, Rabiee M, Moztarzadeh F, Sheikhi M, Tahriri M, Karimi M. Synthesis, characterization and in vitro bioactivity of sol-gel-derived SiO_2–CaO–P_2O_5–MgO bioglass. Mater Sci Eng C. 2009;29:335–40.
33. Krimm S, Tobolsky AV. Quantitative x-ray studies of order in amorphous and crystalline polymers. Quantitative x-ray determination of crystallinity in polyethylene. J Polym Sci. 1951;7:57–76.
34. ISO DOCUMENT 23317. Implants for surgery: in vitro evaluation for apatite-forming ability of implant materials, 2007.
35. ISO DOCUMENT 10993-5. Biological evaluation of medical devices, Part 5, Tests for cytotoxicity: in vitro methods, 1992.
36. Holand W, Beall GH. Glass–ceramic technology. New York: Wiley-Blackwell; 2002.
37. Hench LL, Andersson O. Bioactive glasses. In: Hench LL, Wilson J, editors. An introduction to bioceramics. Advanced series in ceramics. Singapore: World Scientific; 1993. p. 41–62.
38. Filgueiras MR, La Torre G, Hench LL. Solution effects on the surface reactions of a bioactive glass. J Biomed Mater Res. 1993;27:445–53.
39. Peitl O, Zanotto ED, Hench LL. Highly bioactive P_2O_5–NaO–CaO–SiO_2 glass-ceramics. J Non-Cryst Solids. 2001;292:115–26.
40. Bohner M, Lemaitre J. Can bioactivity be tested in vitro with SBF solution? Biomaterials. 2009;30:2175–9.
41. Salman SM, Salama SN, Abo-Mosallam HA. The role of strontium and potassium on crystallization and bioactivity of Na_2O–CaO–P_2O_5–SiO_2 glasses. Ceram Int. 2012;38:55–63.
42. Kivrak N, Tas AC. Synthesis of calcium hydroxyapatite-tricalcium phosphate composite bioceramic powders and their sintering behavior. J Am Ceram Soc. 1998;81:2245.
43. Kamitakahara M, Ohtsuki C, Kozaka Y, Ogata S, Tanihara M, Miyazaki T. Preparation of porous glass–ceramics containing Whitlockite and diopside for bone repair. J Ceram Soc Jpn. 2006;114(1):82–6.
44. El-Meliegy EM, El-Bassyouni GT. Study of the bioactivity of fluorophlogopite–whitlockite ceramics. Ceram Int. 2008;34:1527–32.
45. Banerjee SS, Tarafder S, Davies NM, Bandyopadhyay A, Bose S. Understanding the influence of MgO and SrO binary doping on the mechanical and biological properties of β-TCP ceramics. Acta Biomater. 2010;6:4167–74.